RSC Advances

PAPER

View Article Online
View Journal | View Issue

Cite this: *RSC Adv.*, 2025, **15**, 1690

Synthesis and characteristics of water-based, rosin-modified, polymerized oil based on dehydrated castor oil acid and zinc resinate

Yong-A. Choe, Su-Il Kim, Jong-Hwan Jang and Kyong-Sik Ju *

Received 7th May 2024
Accepted 27th December 2024

DOI: 10.1039/d4ra03350g

rsc.li/rsc-advances

In this study, we synthesized a water-based, rosin-modified, polymerized oil (**WRPO**) *via* an addition and polymerization reaction of dehydrated castor oil (DCO), rosin acid (RA), zinc resinate (ZR) and dehydrated castor oil acid (DCOA). Addition and polymerization reactions at 240 °C, followed by neutralization with ammonia, dissolution into butyl alcohol and subsequent dilution with water, were performed at varying DCOA contents of 10%, 20%, 30%, 35% and 40%. **WRPO** was mixed with butoxymethylmelamine (BMM), a curing agent, at a weight ratio of 80 : 20, and then cured for 2 hours at 130 °C. Structure and thermal characterizations of the prepared **WRPO**s were investigated *via* FTIR spectroscopy, ^{1}H NMR spectroscopy and TGA. Characterization results indicated that when the contents of DCOA and ZR were 35% and 5%, respectively, the obtained **WRPO** exhibited fine water-dispersible stability and excellent physicochemical properties.

1 Introduction

Recently, much attention has been directed toward recyclable bio-resources, such as oil, rosin and lignin, for saving crude oil in the field of organic coatings.[1] Production of high quality synthetic resins, including polyurethane, epoxy and acryl, causes global warming and depletion of the natural resources.[2] Thus, several researchers are focused on the synthesis of paint resin using natural oil, such as alkyd resin and polymerized oil.[3] Polymerized oil has good flexibility and weatherability; hence, it is used for the preparation of wood coatings with some dilutants, such as xylene and white spirit.[4] Solvent-based paints emit a significant amount of organic solvents in the curing process, which causes environmental pollution. In order to address this problem, many scientists have attempted to make oil-based resins that are soluble in water using various methodologies, including the addition of dibasic acids, such as maleic anhydride (MA)[5,6] or fumaric acid (FA),[7] to oil molecules and graft copolymerization using acrylic monomers.[8] MA and FA, which are di-functional monomers, have an unsaturated bond that can raise the carboxyl content of the resin when added to oil molecules, resulting in an improvement in water solubility. However, MA is an oil processing product produced during the oxidation of benzene or *n*-butane,[9,10] and there are few reported research data on biomass-based monobasic acids available for addition to oil. RA is a biomass material, which has a large polycyclic structure and covalent conjugated double bond; thus, it can enhance the hardness, drying ability and water resistance of polymerized oil.[11] Hence, its applications are getting increased annually, especially in organic coatings,[12] adhesives,[13] shape memory polymers,[14] and composites.[15–17] In addition, rosin has one carboxyl group in each molecule, which raises the hydrophilic content. DCOA has two double bonds and one carboxyl group in each molecule, raising the carboxyl content and flexibility through the Diels–Alder reaction. Also, the addition of ZR may facilitate the drying process of the resin by forming a chelate bond with the carboxyl group of the resin. Notably, oil-based water reducible resins exhibit lower performance than solvent-based ones, and thus, in the case of resins with many carboxyl groups, it is common to modify them with BMM.[18,19] Therefore, our work was focused on the manufacturing of **WRPO** using RA and DCOA. The physicochemical characterization of the cured film with BMM was also performed.

High-Tech Research and Development Center, Kim Il Sung University, Pyongyang, Democratic People's Republic of Korea. E-mail: ks.ju1025@ryongnamsan.edu.kp

2 Materials and methods

2.1 Materials

RA was obtained from the Ham-Hung Forest Product Factory; DCO, DCOA, BMM and 25% aqueous ammonia were purchased from the Sunchen Paint Factory, DPR Korean; and butyl alcohol, toluene, ethanol and phenolphthalein, KOH (0.1 N) were obtained from the Shandong Changyu Group Co., Ltd, China.

All the chemicals were technically pure and used as received.

2.2 Preparation of WRPO

Five kinds of **WRPO**s having different DCOA contents (10, 20, 30, 35 and 40%) were prepared with DCO, RA, ZR and DCOA,

Table 1 Formulation of WRPOs

Material	WRPO1	WRPO2	WRPO3	WRPO4	WRPO5
DCO (g)	90	90	90	90	90
RA (g)	180	150	117	96	75
ZR (g)	30	60	3	9	15
DCOA (g)	300	300	90	105	120
Total (g)			300	300	300

according to the formulation shown in Table 1. Defined amounts of DCO, RA and ZR were added to a 500 mL four-necked round flask equipped with a reflux condenser, thermometer, magnetic stirrer and nitrogen inlet, and heated up to 100–105 °C for 0.5 h, and this temperature was then maintained until RA and ZR were completely melted. After that, the temperature of the reactor was enhanced up to 220 °C for 0.5 h and the reaction was performed for 2.5 h, followed by the addition of DCOA into the reactor, and subsequent addition and polymerization at 230–240 °C. The reaction was monitored by periodic determination of the acid value until the acid value dropped to 60–65 mg KOH g^{-1}. After completion of the reaction, **WRPO** was dissolved into butyl alcohol at 100 °C, resulting in the solution containing 80% of non-volatile matter content.

2.3 Curing of WRPO

Naphthenic cobalt and lead drier was added to the as-prepared **WRPO**, and the pH of the solutions was controlled to a final value of 8–8.5 by adding 25% aqueous ammonia and stirring for 0.5 h. After that, the resulting mixture was diluted with water until it contained 45 weight percent of non-volatile content, followed by impregnation painting on a glass plate and subsequent drying at room temperature.

In addition to this, different amounts of BMM (non-volatile ingredients content 60%) was mixed with **WRPO** and stirred for 0.5 h. The additional amount of BMM into **WRPO** has been calculated in terms of the non-volatile content and varied in the range of 5, 10, 15, 20 and 25%. The pH of the reaction mixture was modified with ammonia water until it was weakly alkaline, and diluted so that it contained 45 weight percent of non-volatile content with water. After that, this reaction mixture was painted on the glass plates by impregnation, and cured for 2 h at 130 °C. In the curing process, the following reaction occurred (Scheme 2).

2.4 Characterization

WRPOs were characterized by acid value (ASTM D 1639), saponification value (ASTM D 2689), iodine number (ASTM D 1959) and viscosity (ASTM D 1545). Films formed on the glass plate were characterized by pencil hardness after 48 h (ASTM D 3363), adhesion (ASTM D 3359), flexibility (ASTM D 522), impact strength (ASTM D 2794), acid, alkaline and salt resistance (ASTM D 1308), and water resistance (ASTM D 1647).

The chemical structure of **WRPO**s and the cured film was investigated by infrared analysis with a Nicolet 6700 FTIR spectrophotometer (USA) in the range of 400 and 4000 cm^{-1} and nuclear magnetic resonance spectroscopy (^{1}H NMR). Thermogravimetric analysis (TGA) of the dried films was conducted on a Shimadzu TGA-50H under air atmospheres in the temperature range of 20–800 °C with a 20 °C min^{-1} heating rate.

3 Results and discussion

3.1 Physicochemical properties of WRPOs

When castor oil is dehydrated in the presence of sodium bisulfate and sodium sulfite, its iodine value is increased, which means that the content of the conjugated double bond available for the Diels–Alder reaction to take place is enhanced. RA consists of 90 percent of abietic acid and its derivatives, having reactive functional groups such as a conjugated double bond and carboxyl group.[12] Abietic acid is relatively stable; however, it can be isomerized to levopimaric acid. Levopimaric acid has a high reactive conjugated double bond and facilitates the Diels–Alder reaction to take place with the double bond of DCO. The DCO-rosin addition product is generated as a result of this reaction, and the carboxyl group in RA is inserted into the chain of the polymerized oil, but this provided insufficient hydrophilicity. Hence, we enhanced the hydrophilic group content by supplementary addition of DCOA (Scheme 1). Changes in the acid value and viscosity of **WRPO**s with time after the added DCOA have been plotted in Fig. 1 and 2, respectively.

As shown in Fig. 1, **WRPO**5 has a higher acid value and higher decreasing rate of acid value than **WRPO**1. The decrease of the acid value may be attributed to the residual hydroxyl group in DCO reacting with the carboxyl group of DCOA, and the decarboxylation reaction occurring due to the relatively high reaction temperature. Also, the reason why **WRPO**5 has a higher decreasing rate of the acid value than **WRPO**1 is because the carboxyl group of DCOA is more reactive than that of RA. This is attributed to the steric hindrance effect of the large polycyclic molecule in RA. In addition to this, Fig. 1 indicates that the acid values of all **WRPO**s mostly reach the critical points 2 hours after the reaction started, and no significant change occurred.

As shown in Fig. 2, the viscosity of **WRPO**s increased with the reaction time. All curves in Fig. 2 show a slow increase for the first 4 hours, and then a more rapid increase during the subsequent 2 hours. With consideration of Fig. 1 and 2 indicates that the condensation reaction between the residual hydroxyl and carboxyl group has not progressed to the level of providing a significant effect on the viscosity of **WRPO**s. The subsequent rapid increase after 4 hours is thought to be associated with the formation of a partial ring structure, owing to the addition polymerization. This is because the ring structure formed by the condensation reaction, which has a large number of structural units, provides the flexibility to the chain structure as it is. However, one that is formed by the addition polymerization, which has less structural units, has a detrimental effect on the flexibility, resulting in an increased viscosity. Additionally, the viscosity values of **WRPO** are all higher with a higher content of RA, owing to the steric hindrance effect of the large polycyclic structure of abietic acid. Thus, **WRPO**1 has the highest viscosity compared to the others. The color, acid value, saponification value, iodine number, viscosity and water

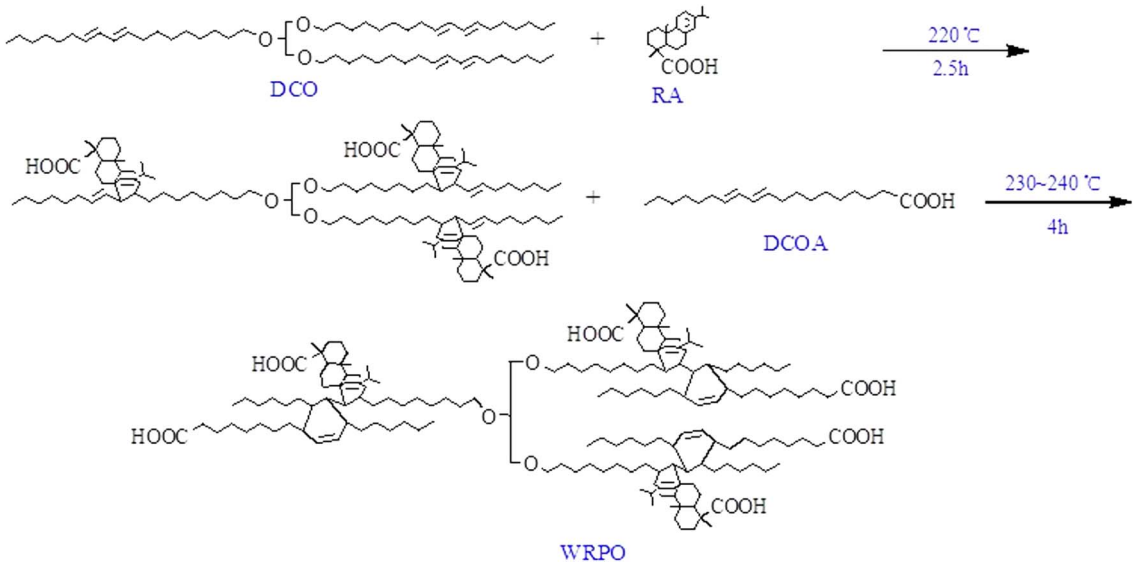

Scheme 1 Polyaddition reaction of **WRPO**.

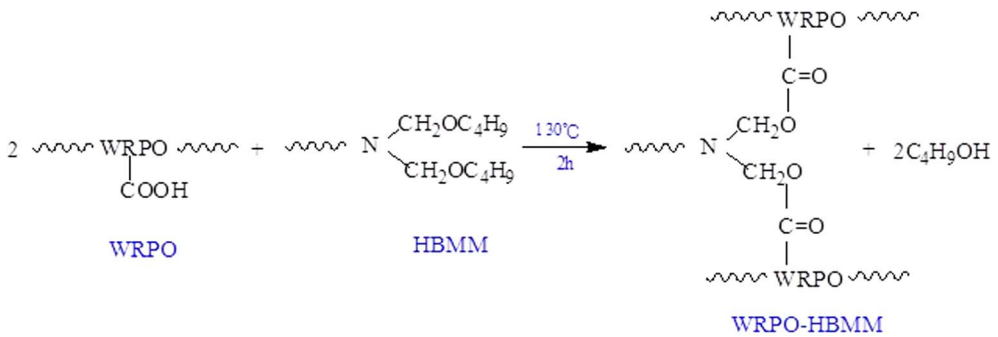

Scheme 2 Curing reaction of **WRPO** with BMM.

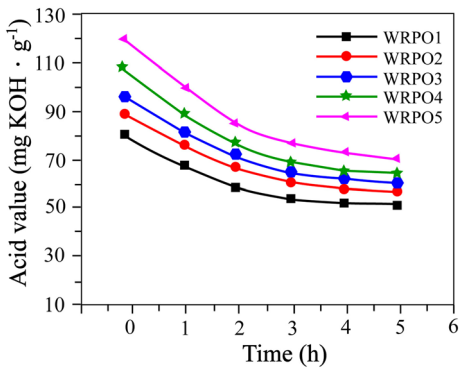

Fig. 1 Acid value change curves of **WRPO**s *versus* time: **WRPO**1 (10% DCOA content), **WRPO**2 (20% DCOA content), **WRPO**3 (30% DCOA content), **WRPO**4 (35% DCOA content), and **WRPO**5 (40% DCOA content).

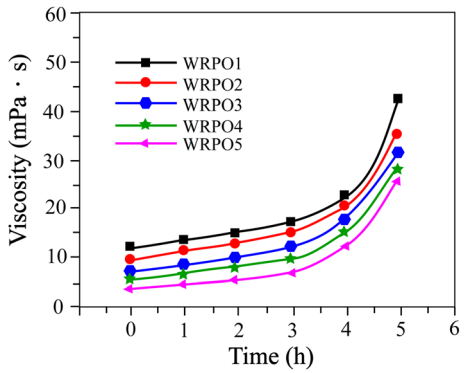

Fig. 2 Viscosity change curves of **WRPO**s *versus* time: **WRPO**1 (10% DCOA content), **WRPO**2 (20% DCOA content), **WRPO**3 (30% DCOA content), **WRPO**4 (35% DCOA content), and **WRPO**5 (40% DCOA content).

dispersion stability of the as-prepared **WRPO**s are listed in Table 2. The long oil alkyd resin reported in ref. 20 was chosen as the reference.

As shown in Table 2, the RA content decreases and the fatty acid content increases with the increase of DCOA content. Thus, both saponification value and iodine number increase, and the

Table 2 Physicochemical properties of WRPOs

Properties	WRPO1	WRPO2	WRPO3	WRPO4	WRPO5	Reference
Color	Dark brown	Dark brown	Dark brown	Dark brown	Dark brown	Dark brown
Acid value (mg KOH g^{-1})	52.8	57.2	60.9	65.9	73.2	9.8
Saponification value (mg KOH g^{-1})	107.4	118.6	128.5	135.4	142.3	119.3
Iodine value (g I_2 100 g^{-1})	74.6	78.5	83.3	85.2	87.8	79.5
Viscosity (mPa s)	43.1	37.5	35.5	32.3	28.6	52.9
Water-dispersible stability (d)	1	7	15	More than 30	25	

increasing rate of the saponification value is higher than that of the iodine number. This is mainly attributed to the double bond of the fatty acid being mostly removed during the addition polymerization. Also, along with the increase of the DCOA content, **WRPO** has the higher acid value and the lower viscosity, resulting in more improved water dispersion stability. This is because DCOA has a higher acid value and more flexibility than RA. However, in the case of the excessively high ZR content, this generates a chelation reaction with the free carboxyl group to form a more partial network structure, leading to poor water dispersion stability.

3.2 Chemical structure of WRPOs

The FTIR spectra of castor oil, DCO, rosin, **WRPO** and the cured film are presented in Fig. 3.

In the FTIR spectrum of DCO, the absorption peak in the range of 3393–3396 cm^{-1} has been weakened and a new peak corresponding to the C=C bond appears at 1586 cm^{-1} compared with that of castor oil. This occurs because of the decrease of the hydroxyl content by the dehydration of water. Also, the FTIR spectrum of DCO shows some additional peaks, including that at 2927 and 2855 cm^{-1}, corresponding to the C–H stretching vibration of the methylene group, 1462 and 725 cm^{-1} corresponding to the scissor and in-plane torsional vibration of the methylene group, 1743 cm^{-1} due to the C=O stretching vibration, and 1251 and 1172 cm^{-1} by the C–O–C stretching vibration. Compared with this, the spectrum of **WRPO** has C–H stretching peaks of the methylene group at 2926 and 2855 cm^{-1}, C–H bending peaks at 1461 and 726 cm^{-1}, C=O stretching peak of the ester group at 1735 cm^{-1} and C–O–C stretching vibration peaks

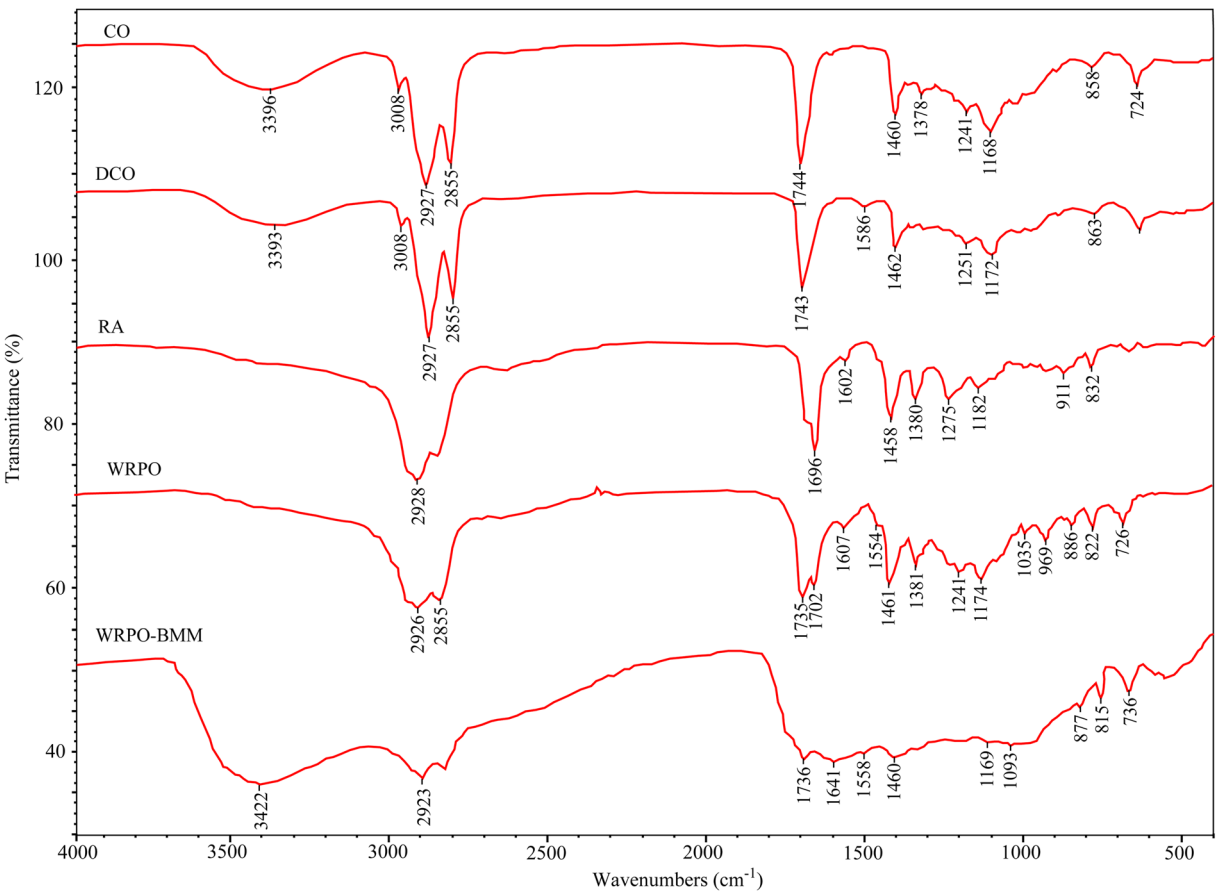

Fig. 3 FTIR spectra of CO, DCO, RA, **WRPO** and **WRPO**-BMM.

at 1241 and 1174 cm^{-1}. The spectrum of RA displays a stretching peak corresponding to the C=O bond of the carboxyl group at 1696 cm^{-1}.[21] Thus, two peaks at 1735 and 1702 cm^{-1} in the spectrum of **WRPO** can be considered to refer to the carboxyl group of DCO and RA, respectively.

Also, the absorption peak of the C=C bond appeared at 1602 cm^{-1} in the FTIR spectrum of RA was observed at 1607 cm^{-1} for **WRPO**. However, there was no peak corresponding to the C=C bond of DCO near 1586 cm^{-1} in the spectrum of **WRPO**, which indicates that the addition and self-polymerization reaction predominantly proceed in the conjugated double bond of DCO. The absorption peak responsible for the hydroxyl group of DCO at 3393 cm^{-1} was not observed in the spectrum of **WRPO**, which demonstrates that the residual hydroxyl group of DCO has successively reacted with the carboxyl group to form an ester group. Moreover, a new absorption peak at 969 cm^{-1} can be assigned to the stretching vibration of the tertiary C–C bond generated by the addition reaction.

For further structural characterization, we conducted NMR spectroscopic analysis. Fig. 4 displays the NMR spectra of RA, **WRPO** and the cured film.

The NMR spectrum of **WRPO** shows peaks due to the proton of the end methyl group of the aliphatic chain at 0.82–0.87 ppm, the proton adhered to the adjacent carbon atom of the end methyl group at 1.57–1.61 ppm, and the proton of all methyl groups existing in the aliphatic chain at 1.25–1.26 ppm. In the spectrum of **WRPO**, there exist three peaks (a, b and e) due to the proton of CH next to the unsaturated carbon atom, and peak d corresponding to the proton of the tertiary carbon appeared by the addition of abietic acid into the aliphatic chain in the range of 2.34–2.56 ppm. Also, peak (f) at 4.15–4.38 ppm is assigned to the proton of the methylene group in glyceride, 5.15–5.21 ppm indicates the proton of the unsaturated carbon in the aliphatic acid, and peak (c) at 5.32–5.38 ppm corresponds to the unsaturated carbon of abietic acid.[22,23]

The spectrum of the cured film of **WRPO** shows two additional peaks corresponding to the butoxy group of BMM and the methylene group between the nitrogen and oxygen atoms at 3.12–3.23 ppm and 5.12–5.15 ppm, respectively.[24]

3.3 Drying of WRPOs

In order to investigate the drying process of **WRPO** at different DCOA and ZR contents, cobalt and lead naphthenate drier were added at 0.13% and 0.45% of the weight of oil, respectively, followed by flow painting on the glass plate, and dried. Table 3 shows the set-to-touch, surface, and thorough drying times of **WRPO**s and the reference resin.

Table 3 indicates that the drying times of **WRPO**s are longer than that for the reference resin, which can be considered to be from the greater latent heat of vaporization of water than organic solvent and to the relatively small molecular weight of **WRPO**s. As can be seen from the table, the drying time increases with increasing DCOA content. This is mainly due to the hydrophilicity of DCOA, leading to an increase in the time necessary for drying the **WRPO**s, and also partly due to its small molecular weight. Furthermore, the drying time decreases with increasing ZR content, which can be attributed to the acceleration of the three-dimensional network formation due to the chelate reaction between zinc and the free carboxyl group.

3.4 Properties of WRPOs

3.4.1 Physical properties. The physical properties of **WRPO**s are listed in Table 4. The adhesion, pencil hardness, impact strength and flexibility are all important physical properties of paint resins. As shown in the table, the adhesion values of the **WRPO**s are all excellent because their main constituents are aliphatic compounds. The impact strength of the **WRPO**s has a relatively high value since the intermolecular interaction is strengthened due to the addition of the large aromatic rosin

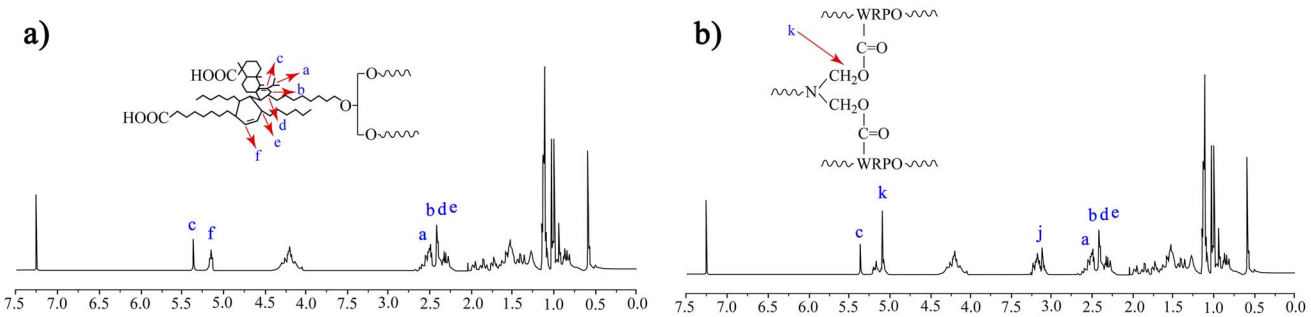

Fig. 4 ^{1}H NMR spectra of **WRPO** (a) and its cured film by BMM (b).

Table 3 Drying time of **WRPO**s

Resins	**WRPO1**	**WRPO2**	**WRPO3**	**WRPO4**	**WRPO5**	Resin (reference)
Set-to-touch (min)	240	270	210	180	150	80
Surface (h)	18	22	12	10	9	5
Thorough (h)	32	38	26	24	19	6.5

Table 4 Physical properties of dried WRPOs

Property	**WRPO**1	**WRPO**2	**WRPO**3	**WRPO**4	**WRPO**5	Resin (reference)
Adhesion (%)	100	100	100	100	100	100
Pencil hardness	1B	1B	2B	2B	2B	1H
Impact strength (N m)	40	40	40	40	40	50
Flexibility (mm)	1	1	1	1	1	1

molecule, but this is lower than that for the reference resin. Moreover, the pencil hardness decreases with the increase of the DCOA content, which can be attributed to the increase of the flexible chain content.

Different percentages of BMM (non-volatile content 60%) were added to **WRPO**4, which has the best water dispersion stability, at values of 5, 10, 15, 20 and 25% according to solid weight, and homogeneously mixed by stirring for 0.5 h. A 25% ammonia water solution was added to the mixture to increase the pH until it was weakly alkaline, and the resulting reactant was diluted until the non-volatile content reached 45%, followed by impregnation painting on a glass plate and subsequent curing at 130 °C for 2 h. Table 5 shows the measurement results of the adhesion, pencil hardness, impact strength and flexibility for the as-obtained film in the case of different BMM contents.

As shown in the table, the pencil hardness of **WRPO**4 increases with the increase in the BMM content, but the impact strength and flexibility increase and then decrease. This occurs because the excess addition of BMM leads to signify brittleness of the resin.

3.4.2 Chemical resistance of WRPOs. Alkaline, acid, salt and water resistances of **WRPO**s have been tested in 0.1 N KOH, 0.1 M H_2SO_4, 5% NaCl and ordinary water, respectively. Table 6 shows the appearance of **WRPO**s 24 hours after being immersed in the relevant solutions.

As listed in Table 6, with the increase of the DCOA content, the acid, salt and water resistances of **WRPO** decrease owing to the existence of the hydrophilic group and to the decreased molecular weight. On the other hand, the alkaline resistance of all **WRPO**s shows poor behavior due to the free carboxyl group that still remained after drying. ZR provides **WRPO** with more enhanced chemical resistance by forming a chelate bond with the carboxyl group of the main chain during the curing process. Thus, the acid, salt and water resistances of **WRPO** all increase with the increase of the ZR content.

The testing results of the chemical resistance of **WRPO**4 cured with different amounts of BMM using the method mentioned above are listed in Table 7. From the table, it can be seen that the alkaline resistance of **WRPO**4 increases with the increase of the BMM content, but shows no apparent improvement after 20%. This phenomenon can be explained by the crosslink reaction conducted between the free carboxyl group of **WRPO** and methyl group of BMM, resulting in an increase of the intermolecular interaction energy (due to the increased molecular weight) and removal of the unreacted carboxyl group.

3.4.3 Thermogravimetric analysis (TGA). For evaluation of the thermal decomposition properties of **WRPO**s together with the content of DCOA, TGA has been performed. The TG & DTG curves obtained under the temperature range of 20–800 °C and the heating rate of 20 °C min^{-1} are presented in Fig. 5.

As shown in Fig. 5, the decomposition of **WRPO**s consists three main stages. The first stage contains the evaporation of the high boiling point solvent and liberation of the unreacted curing agent. The second stage is a rapid decomposition process due to dissociation of covalent bonds, such as C–O and C–C, and the third stage can be considered as the decomposition process of the residual species.

Table 5 Physical properties of WRPOs

Property	**WRPO**4–BMM5	**WRPO**4–BMM10	**WRPO**4–BMM15	**WRPO**4–BMM20	**WRPO**4–BMM25
Adhesion (%)	100	100	100	100	100
Pencil hardness	1B	1H	3H	3H	4H
Impact strength (N m)	50	50	50	50	40
Flexibility (mm)	1	1	1	1	3

Table 6 Chemical resistance of WRPOs[a]

Type of media	**WRPO**-1	**WRPO**-2	**WRPO**-3	**WRPO**-4	**WRPO**-5	Resin (reference)
Alkali (0.1 N KOH)	4	4	4	4	4	2
Acid (0.1 M H_2SO_4)	1	1	2	1	1	1
Salt (5%, w/w NaCl)	1	2	2	1	1	1
Water (cold)	1	2	2	1	1	1

[a] 1—no effect, 2—wrinkle, 4—film removed.

Table 7 Chemical resistance of **WRPO**s according to BMM[a]

Type of media	**WRPO**4–BMM5	**WRPO**4–BMM10	**WRPO**4–BMM15	**WRPO**4–BMM20	**WRPO**4–BMM25
Alkali (0.1 N KOH)	4	3	3	2	2
Acid (0.1 M H_2SO_4)	1	1	1	1	1
Salt (5%, w/w NaCl)	1	1	1	1	1
Water (cold)	1	1	1	1	1

[a] 1—no effect, 2—wrinkle, 3—blistering, 4—film removed.

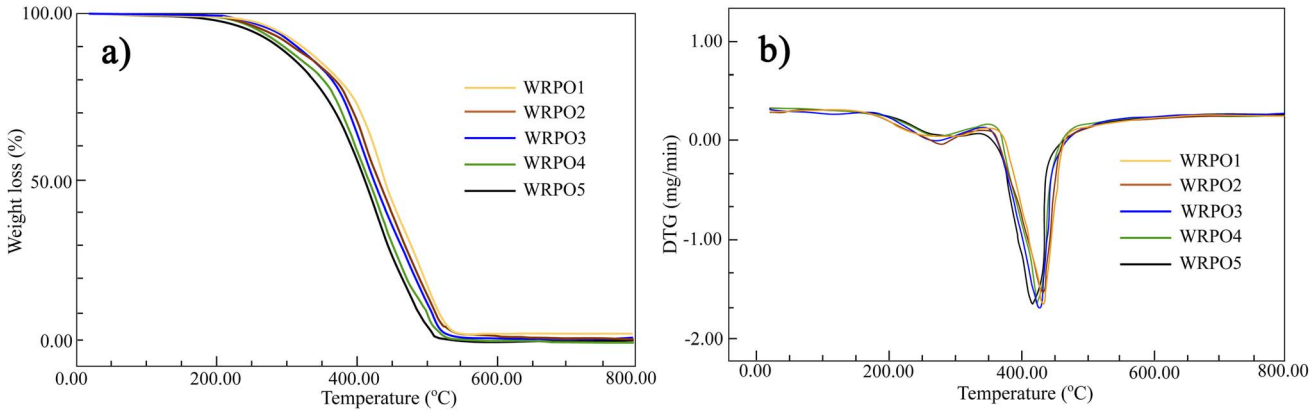

Fig. 5 TGA results of **WRPO**s: (a) TGA curves, (b) DTG curves.

It is common that the temperature at which half of the weight loss occurs is used for the estimation of the thermal stability of polymer systems.[25] From Fig. 5a, it can be seen that the temperature at which 50% weight loss occurs decreased from 432 °C to 412 °C due to the increase in the DCOA content. Also, the temperature at which the maximum weight loss occurred in the DTG curves of **WRPO**s, as shown in Fig. 5b, was measured at 432, 426, 419, 416 and 412 °C for **WRPO**1–**WRPO**5 containing 10, 20, 30, 35 and 40% of DCOA content, respectively.

The TGA results mentioned above indicate that DCOA has a negative effect on the thermal stability of **WRPO**. This is likely because of the corresponding decrease in the amount of large aromatic rosin structure. The TGA results also show that the thermal stability of the six-membered alicyclic ring structure generated by the addition of DCOA is lower than that of the large polycyclic structure of RA.

4 Conclusion

In this work, we prepared **WRPO**s by the addition and polymerization reaction of DCO, RA, ZR and DCOA, and dried them with BMM for 2 h at 130 °C. The chemical structure of as-prepared resin was investigated by FTIR and NMR spectroscopic analysis. Characterization results indicated that **WRPO** prepared under the condition when the DCOA and ZR contents were 35 and 5%, respectively, has the best water dispersion stability and physicochemical properties. The present work demonstrates the ability to prepare water-based paint resins by using natural materials containing mono-functional acids. This achievement may be effectively used to manufacture environmentally friendly "green coatings" based on biomass, although some of the physical and chemical performances of the prepared resin are lower than those of synthetic resin.

Data availability

The data that support the findings of this study are available from the corresponding authors upon reasonable request.

Conflicts of interest

The authors declare that they have no known competing financial interests or personal relationships that could have appeared to influence the work reported in this paper.

Acknowledgements

This work is supported by the National Committee of Science and Technology in DPR Korea.

References

1 X. Huang, Bio-based thermosetting epoxy foams from epoxidized soybean oil and rosin with enhanced properties, *Ind. Crops Prod.*, 2019, **139**, 111540.
2 G. Liu and G. Wu, Synthesis, Modification and Properties of Rosin-Based Non-Isocyanate Polyurethanes Coatings, *Prog. Org. Coat.*, 2016, **101**, 461–467.

3 F. Chardon, M. Denis and C. Negrell, Hybrid alkyds, the glowing route to reach cutting-edge properties?, *Prog. Org. Coat.*, 2021, **151**, 106025.
4 A. Philip and P. E. Schweitzer, *Paint and Coatings: Applications and Corrosion Resistance*, CRC press, 2006.
5 A. I. Aigbodion, Utilization of maleinized rubber seed oil and its alkyd resin as binders in waterborne coatings, *Prog. Org. Coat.*, 2003, **46**, 28–31.
6 C. F. Uzoh, Synthesis of rubber seed oil waterborne alkyd resin from glucitol, *J. Coat. Technol. Res.*, 2019, **16**(6), 1727–1735.
7 E. U. Ikhuoria, Preparation and characterisation of water-reducible alkyds with fumarized rubber seed oil, *Prog. Org. Coat.*, 2005, **52**, 238–240.
8 Ö. zge Naz, Is. ıl Acar and G. Güclu, Synthesis of four-component acrylic-modified water-reducible alkyd resin: investigation of dilution ratio effect on film properties and thermal behaviors, *J. Coat. Technol. Res.*, 2017, **14**(1), 117–128.
9 N. Araji, D. D. Madjinza, G. Chatel, A. Moores, F. Jérôme and K. D. O. Vigier, Synthesis of maleic and fumaric acids from furfural in the presence of betaine hydrochloride and hydrogen peroxide, *Green Chem.*, 2017, **19**, 98–101.
10 R. Wojcieszak, Recent developments in maleic acid synthesis from bio-based chemicals, *Sustainable Chem. Processes*, 2015, **3**(9), 1–11.
11 A. Arthur *Tracton, Coatings Materials and Surface Coating*, CRC press, 2007.
12 R. A. El-Ghazawy, Rosin based epoxy coating: Synthesis, identification and characterization, *Eur. Polym. J.*, 2015, **69**, 403–415.
13 B. Kollbe Ahn, UV-curable pressure-sensitive adhesives derived from functionalized soybean oils and rosin ester, *Polym. Int.*, 2013, **62**, 1293–1301.
14 T. Li and X. Liu, Bio-based shape memory epoxy resin synthesized from rosin acid, *Iran. Polym. J.*, 2016, **25**, 957–965.
15 Z. Xu Feng, Curing kinetics and mechanical properties of bio-based composite using rosin-sourced anhydrides as curing agent for hot-melt prepreg, *Sci. China: Technol. Sci.*, 2017, **60**(9), 1318–1331.
16 Y. Liu, Synthesis of multifunctional monomers from rosin for the properties enhancement of soybean-oil based thermosets, *Sci. China: Technol. Sci.*, 2017, **60**(9), 1332–1338.
17 M. Yang, X. Y. Chen, H. X. Lin, C. R. Han and S. F. Zhang, A simple fabrication of superhydrophobic wood surface by natural rosin based compound *via* impregnation at room temperature, *Eur. J. Wood Wood Prod.*, 2018, **76**, 1417–1425.
18 S. Kewaldas Dhoke, Formulation and performance study of low molecular weight, alkyd-based waterborne anticorrosive coating on mild steel, *Prog. Org. Coat.*, 2008, **62**, 183–192.
19 A. Torlakoğlu, Alkyd–amino resins based on waste PET for coating applications, *Waste Manage.*, 2009, **29**, 350–354.
20 Y.-A. Choe, Synthesis and characterizations of high oil length alkyd resin with dehydrated castor oil and acrylic pimaric acid, *Chem. Phys. Lett.*, 2022, **805**, 139934.
21 X. Yan, Synthesis and properties of polyester-based polymeric surfactants from diterpenic rosin, *Ind. Crops Prod.*, 2017, **108**, 371–378.
22 E. F. Assanvo, Synthesis, characterization, and performance characteristics of alkyd resins based on Ricinodendron heudelotii oil and their blending with epoxy resins, *Ind. Crops Prod.*, 2015, **65**, 293–302.
23 M. M. Bora, Karanja (Millettia pinnata (L.) Panigrahi) seed oil as a renewable raw material for the synthesis of alkyd resin, *Ind. Crops Prod.*, 2014, **61**, 106–114.
24 S. M. Caki'c, Glycolyzed poly(ethylene terephthalate) waste and castor oil-based polyols for waterborne polyurethane adhesives containing hexamethoxymethyl melamine, *Prog. Org. Coat.*, 2015, **78**, 357–368.
25 Q. Ge, H. L. Wang, Y. She, S. W. Jiang, M. Y. Cao, L. F. Zhai and S. T. Jiang, Synthesis, Characterization, and Properties of Acrylate-Modified Tung-Oil Waterborne Insulation Varnish, *J. Appl. Polym. Sci.*, 2015, **132**, 41608.